AIAA JOURNAL
Vol. 42, No. 11, November 2004

Accounting for Laminar Run and Trip Drag in Supersonic Cruise Performance Testing

Aga M. Goodsell*
NASA Ames Research Center, Moffett Field, California 94035-1000
and
Robert A. Kennelly Jr.†
Objective Insights, Inc., Palo Alto, California 94309-8401

Recent experimental assessment of cruise performance for a supersonic transport has led to reevaluation of some time-honored techniques for trip drag correction. Two wind-tunnel tests were conducted on a wing/body configuration at Mach 2.4 and Reynolds number 6.4×10^6. A method for determining corrections to the drag near the cruise angle of attack is presented. These corrections account for the trip drag associated with attempts to induce boundary-layer transition and for the effect of any laminar flow that persists on the model. Extensive flow visualization using a subliming chemical revealed that the boundary-layer trip was not consistently effective. Flow over a portion of the upper wing surface exhibited delayed transition for even the largest trip heights tested. Laminar run corrections based on measured transition locations were computed using flat-plate skin-friction formulas. Once corrected for laminar run, the drag was constant for small trip heights ("drag plateau") before linearly increasing with trip height. Therefore, a trip drag correction is required only for those trip heights beyond the plateau. It is concluded that correction for laminar run is essential and must precede evaluation of trip drag. Neither correction is negligible at the level of accuracy desired.

Nomenclature

b	=	wing span
C_D	=	drag coefficient
C_f	=	local skin-friction coefficient
C_L	=	lift coefficient
C_m	=	pitching moment coefficient
C_p	=	pressure coefficient
c	=	local wing chord
d	=	trip disk diameter
k	=	trip height
Re_k	=	roughness height Reynolds number based on local flow conditions at top of roughness element (but without the element present)
Re_x	=	streamwise Reynolds number based on distance x from leading edge to trip and freestream flow conditions
u	=	streamwise velocity
x	=	Cartesian coordinate in freestream direction
y	=	Cartesian coordinate in spanwise direction
z	=	local coordinate normal to surface

Introduction

NASA'S High Speed Research Program (HSRP) sought to establish the technology foundation to support the U.S. transport industry's decision for an environmentally acceptable, economically viable, 300-passenger, 5000-n mile (9260-km), Mach 2.4 aircraft.[1] To realize this ambitious goal, accurate and precise drag measurements are fundamental aerodynamic testing requirements. The value of supersonic cruise drag, for instance, is desired to within ±0.5 counts (±0.00005 C_D) with 80% confidence. This uncertainty is equivalent to ±3000 lb (±1361 kg) in takeoff weight or approximately ±15 passengers.

Most of the supersonic HSRP testing has been conducted in the Unitary Plan Wind Tunnel (UPWT) at NASA Langley Research Center.[2] At achievable chord Reynolds numbers of only a few million, extensive regions of laminar flow exist on the model, whereas for full-scale Reynolds numbers on the order of 200×10^6, the flow is expected to be turbulent over most of the wing. To more closely simulate flight conditions, it was desired to fix the location of the boundary-layer transition near the leading edge using a row of small roughness elements.[3,4] However, applied roughness is not always effective in producing prompt transition, and it sometimes creates additional drag; both of these problems have been observed in HSRP supersonic testing. This paper examines some of the issues that arise when fixing transition in high-speed performance testing. An improved method for estimating the effect of laminar run, which reduces the measured drag, and the effect of the artificial trip, which increases it, is presented.

Background

The technique of adding roughness (e.g., wire, grit, glass beads, epoxy disks) to wind-tunnel models to trip the flow has been used at least since World War II.[5,6] In subsonic flow, prompt transition (immediately behind the trip) can be obtained with trips small enough to incur little or no additional drag,[7] but this is not the case at supersonic and hypersonic speeds. Braslow and coworkers[7] developed criteria to estimate the trip size and location required to induce prompt transition over a range of Mach numbers using Re_k as the correlation parameter. With a sufficiently large trip height, transition begins to move forward of its natural transition location. The value of Re_k corresponding to this trip height is referred to as the critical value.

In their wind-tunnel tests, Braslow et al.[7] used a narrow band of sparsely distributed grit particles to trip the flow. At subsonic speeds, when the critical value of Re_k is reached, transition moves quickly up to the location of the trips. For particles with a height-to-width ratio equal to approximately 1, such as grit or spherical beads, the critical value of Re_k was found to be about 600. At supersonic speeds, Braslow et al. found that transition tends to be delayed; prompt transition may require much larger values of Re_k than the critical value. For Mach numbers below 3.0, trip heights corresponding to $Re_k = 600$ can induce prompt transition if Re_x is greater than a

Received 8 January 2000; accepted for publication 27 May 2003.

*Aerospace Engineer, Mail Stop 258-1; Aga.M.Goodsell@nasa.gov. Senior Member AIAA.
†Senior Consultant, P.O. Box 18401; RAKennelly@ObjectiveInsights.com.

certain minimum value that increases with freestream Mach number. However, it may sometimes be necessary to use a trip height that would result in additional drag in order to satisfy these criteria.

Braslow et al. assert that the drag caused by the addition of roughness is proportional to the particle frontal area and to the average dynamic pressure over the particle. When the height of the particle is smaller than the boundary-layer thickness, the average dynamic pressure on the particle varies with height. The drag on the particle falls rapidly as its height and the average dynamic pressure together approach zero. On the other hand, for trip sizes on the order of the boundary-layer height and greater, the average dynamic pressure over the particle is approximately constant, and so the drag grows in proportion to the frontal area. For grit particles whose frontal area varies with the square of the grit dimension, e.g., spheres or sand grains, a straight-line fit of the drag data vs k^2 is felt to be appropriate. To represent turbulent flow from the location of the trip, but in the absence of a trip, an extrapolation is made to zero trip height. The trip drag for a specific trip height is equal to the difference between the measured drag and the extrapolated value at zero height. The trip drag is subtracted from the measured value to obtain the corrected drag of the model.

Another approach to assessing trip drag was proposed by Vaucheret,[8] who conducted a series of wind-tunnel tests on a delta-wing model at supersonic speeds. A single row of glass beads was used to induce transition. The diameter of the beads was varied to obtain drag as a function of trip size. He observed delayed transition on the model for the smallest bead diameters, as determined by flow visualization. An estimated laminar run correction based on measured transition locations was added to the measured drag before determining the magnitude of the trip drag. A drag plateau in the corrected data was observed for those trip sizes that were not immediately effective in tripping the flow. The existence of a drag plateau eliminates the need to extrapolate the data to zero trip height. Vaucheret concluded that the beads did not begin to produce additional drag until they were large enough to cause prompt transition on the wing. The trip drag is the difference between the measured drag and the plateau value. Others including Fallis[9] and Daugherty[10] have also seen a drag plateau in experimental data obtained at supersonic speeds. However, it is important to note that these researchers did not apply a laminar run correction to their data, and so the resulting drag plateaus did not extend all the way down to zero trip height.

This paper presents results that differ somewhat from the approach to trip drag analysis described by Braslow et al. The previous work by Vaucheret has proven to be more applicable in assessing trip drag here. Some of the discrepancy between the historical and current work may be due to differences in model geometry and the resulting pressure distributions. The current model has blunt leading edges on the highly swept inboard region and sharp leading edges outboard. The transition behavior and response to the boundary-layer trips of the flow in the outboard region, which has gentle pressure gradients, is similar to that observed in the historical tests. However, the inboard airfoil sections produce a rapid expansion around the leading edge followed by a broad pressure peak. The resulting pressure distribution causes the flow to have a different behavior in the inboard region from that in the outboard region. The blunt inboard leading edge may also support a turbulent attachment line, further complicating the interpretation of the results.

Experiment

Two wind-tunnel tests were conducted using the baseline HSRP model in the NASA Langley UPWT (January 1997 and May 1999). The first test sought to establish the cruise performance of the configuration, including appropriate drag corrections, and the objective of the second test was to repeat parts of the earlier test and to obtain additional data on laminar run and trip drag corrections. The HSRP baseline configuration has a cranked-delta wing whose highly swept (71 deg) inboard panel has a blunt leading edge. Outboard of the planform break, the 52-deg-swept leading edge is sharp. The results for the wing/body configuration (no nacelles or tails) at the supersonic cruise Mach number of 2.4 are the focus of the present analysis. The wind-tunnel Reynolds number was 4×10^6/ft (13.1×10^6/m), corresponding to a wing mean-chord Reynolds number of 6.4×10^6.

Epoxy disks, 0.050 in. (1.27 mm) in diameter, were applied to the fuselage and wing to induce boundary-layer transition.[3] The disks on the fuselage were located 1.0 in. (2.54 cm) behind the nose with a 0.1-in. (2.54-mm) center-to-center spacing, and their height remained constant at 0.012 in. (0.305 mm) throughout the test. The epoxy disks on the upper and lower wing surfaces were applied 0.6 in. (1.52 cm) downstream of the leading edge, with a 0.2-in. (5.08-mm) center-to-center spacing. In the first wind-tunnel test, the height of the disks was varied from 0.006 to 0.017 in. (0.152 to 0.432 mm). Two smaller disk heights were added in the second test, 0.002 in. (0.0508 mm) and 0.004 in. (0.102 mm), and the heights up through 0.012 in. (0.305 mm) were repeated. Trip disk heights were sampled to monitor size and consistency. It was required that the average height be within 0.0005 in. (0.0127 mm) of the nominal value specified and that the standard deviation of the heights be less than 0.00025 in. (0.00635 mm).

Forces and moments were measured over a range of angles of attack between −4 and 10 deg. The Langley Unitary Tunnel (UT) 65-A and 65-B internal strain-gauge balances were used for the first and second tests, respectively. The balance capacities (and calibrated accuracies) are as follows: normal force = 800 lb or 3558 N [±0.1% full scale (FS)], axial force = 60 lb or 267 N (±0.25% FS), and pitching moment = 2000 in. · lb or 226 N · m (±0.1% FS). At least three repeat runs were conducted for each trip height to reduce the uncertainty in the drag data. The drag polar for each run or set of repeats was represented by a seventh-order least-squares polynomial fit through the data points (Fig. 1). Bias errors are for the most part irrelevant here, but uncertainty from random sources, the "test repeatability," will play a role in the interpretation of our laminar run and trip drag results. Considering short-term effects only, 95%-confidence intervals for different portions of the drag polars were estimated by fitting each run separately, interpolating to find C_D at a specified angle of attack, and then computing the sample mean and standard deviation of these quantities. Assuming that the interpolants are normally distributed, the precision uncertainty P of the mean C_D is $P_{C_{D(\text{mean})}} = \pm t S_{C_D}/(\sqrt{N})$, where S_{C_D} is the standard deviation of the C_D values and t is read from the Student's t distribution table for 95% confidence and $N-1$ degrees of freedom.[11] Here, $N = 3$ for a typical group of repeat runs and thus $t = 4.30$. The result near the cruise angle of attack is ±0.15 counts.

In addition to the short-term test repeatability, there is some uncertainty associated with different trip disk applications for the same nominal trip height, despite efforts to standardize the height, location, and shape of the disks. Consistency of trip application may be

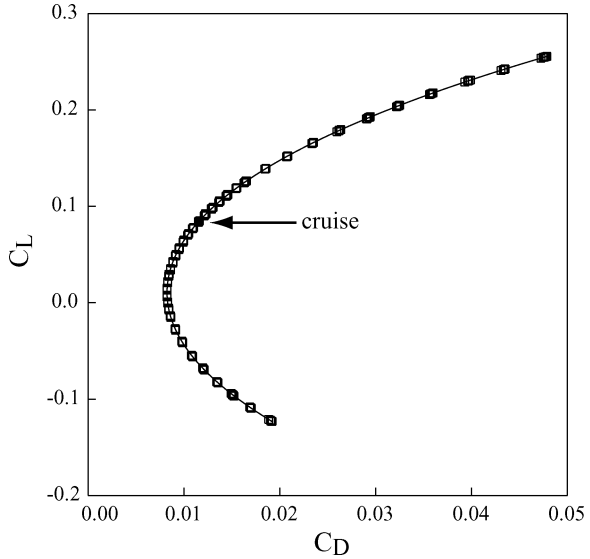

Fig. 1 Drag polar at Mach 2.4 for $k = 0.012$ in. (0.305 mm) represented by seventh-order polynomial fit to six repeat runs.

evaluated by examining "within-test" repeats, where a trip configuration was tested, removed, and later retested. Two such replications are available: disk heights of 0.012 in. (0.305 mm) were repeated during both test entries, yielding shifts in average, interpolated drag between the two applications of about 0.1 and 0.3 counts in the first and second tests, respectively. These shifts are not very different from what one would expect to see on short-term repeatability grounds alone.

Flow visualization with a subliming solid was used to indicate transition[12,13] at the cruise angle of attack, 3.5 deg. In several locations on the wing, a disk was isolated by removing two or three of its neighbors on each side; this makes the wake of an individual disk more visible. The sublimation material was a saturated solution of fluorene ($C_6H_4CH_2C_6H_4$) in a Freon solvent. An airless spray gun was used to apply the material. Two 70-mm still cameras with wide-angle lenses, one on each side of the test section, were used to record the upper and lower wing surfaces. Once the tunnel conditions had stabilized, pictures were taken at regular intervals until most of the material had sublimed, about 20–60 min. Further details of the flow visualization setup, process, and, application are provided by Kennelly and Goodsell.[14]

Results

Initial Analysis

In the initial analysis of the data from the first wind-tunnel test, the approach of Braslow et al.[7] was used to determine the trip drag at cruise. Drag values at $C_L = 0.0845$, corresponding to 3.5-deg angle of attack, were plotted as a function of disk height for the free transition case and for trip heights between 0.008 and 0.014 in. (0.203 and 0.356 mm); see Fig. 2. Prompt transition was expected for these heights based on previous HSRP investigators' conclusions and because Braslow et al.'s supersonic trip height criteria were met: the disks were located at $Re_x = 2 \times 10^5$ and $Re_k > 600$. Re_k values were based on laminar boundary-layer properties from a compressible flat-plate calculation. Strongly "scrubbed" regions observed immediately downstream of the trip disks were interpreted to be indicative of prompt transition (Fig. 3).

The next step in the analysis, extrapolation to zero trip height, was problematic. Following Braslow et al.'s reasoning, the drag is proportional to the frontal area of the epoxy disks ($d \times k$). Because the diameter of the disks is constant, the drag should vary linearly with height. However, a linear extrapolation to zero trip height almost passes through the measured drag for free transition (Fig. 2). The result of this extrapolation, intended to represent fully turbulent flow on the wing, is suspect because the free transition drag, with large regions of laminar flow, should be significantly lower than for the turbulent case. A quadratic extrapolation (suggested by some) provides a more believable value for fully turbulent drag with no trips, but it does not fit the data especially well (Fig. 2). The linear extrapolation results in a trip drag estimate of 5.5 counts for disk height 0.012 in. (0.305 mm), whereas quadratic extrapolation yields 3.0 counts for the same height. The difference between these trip drag estimates (2.5 counts) reflects a larger uncertainty than can be tolerated.

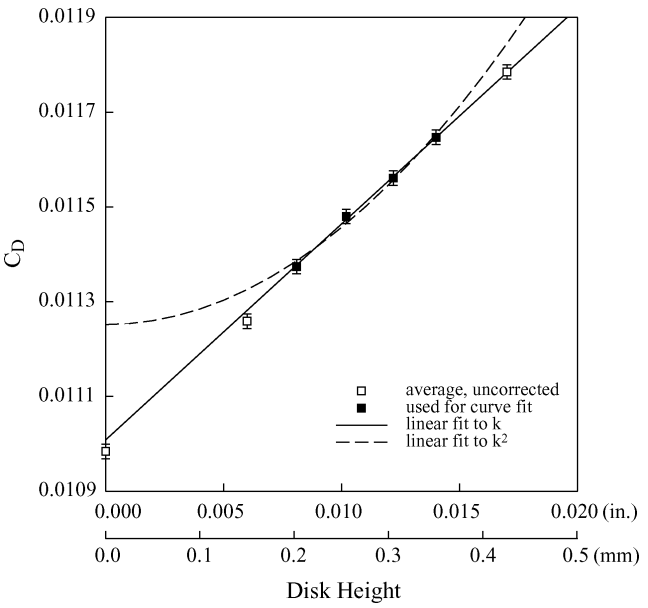

Fig. 2 Drag at average cruise lift ($C_L = 0.0845$) as a function of trip height, used for initial analysis of trip drag.

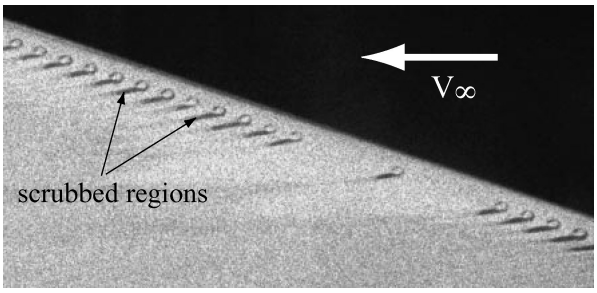

Fig. 3 Sublimation image showing scrubbed regions on the inboard, upper surface, $k = 0.012$ in. (0.305 mm), early in the run.

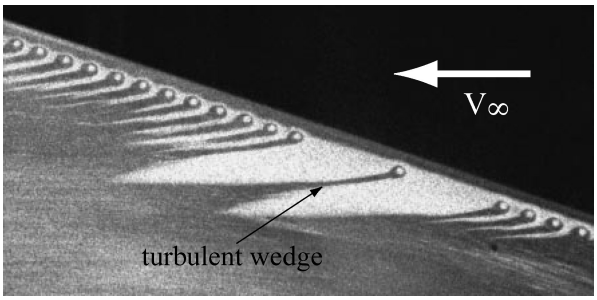

Fig. 4 Sublimation image showing delayed turbulent wedges on the inboard, upper surface, $k = 0.012$ in. (0.305 mm), later in the run.

Revised Interpretation of Flow Visualization Images

The difficulty in estimating trip drag using the approach of Braslow et al.[7] suggested a second, more careful look at the sublimation images. We have concluded that the scrubbed regions immediately downstream of the disks were mistakenly interpreted as evidence of transition. That transition actually occurs somewhat behind the trip is evident from the characteristic 10–15-deg (included angle) turbulent wedges visible downstream in many of the sublimation images; see Figs. 3 and 4. This revised interpretation is supported by the skin-friction data obtained by Drake.[15] In his measurements of the streamwise component of skin friction behind cylindrical protuberances, regions of high shear were observed in the near wake. These are presumably caused by the horseshoe vortices shed by the disks.[16,17] For the smaller disk heights, the characteristic spreading zone of turbulent skin friction does not appear until somewhat farther downstream. Transition on the wing is actually delayed, particularly in the inboard region of the upper surface, for even the largest disk heights tested, and a laminar run correction based on measured transition location must be applied to the drag data before the trip drag can be evaluated.

To measure the transition locations, a series of sublimation images for each trip height were digitally scanned. Because the sublimation material cannot be sprayed with perfect uniformity and because skin friction (and mass transport at the surface) varies over the surface of the wing, different images in each run series are used to locate transition on different portions of the wing. Transition locations were mapped using three specific features: 1) In the outboard region of the upper surface and on the entire lower surface, distinctive turbulent wedges appear either immediately or a short distance downstream of the disks; see Figs. 5 and 6. On the upper,

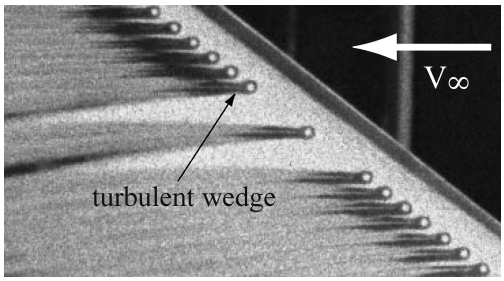

Fig. 5 Sublimation image of turbulent wedges on the outboard, upper surface, $k = 0.012$ in. (0.305 mm).

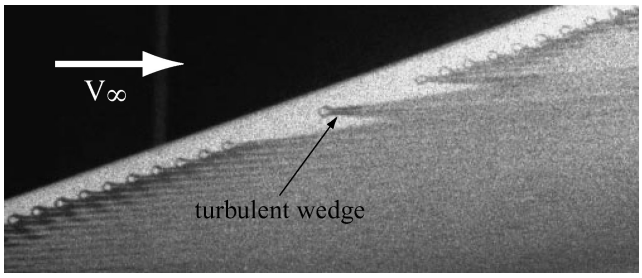

Fig. 6 Sublimation image of turbulent wedges on the inboard, lower surface, $k = 0.012$ in. (0.305 mm).

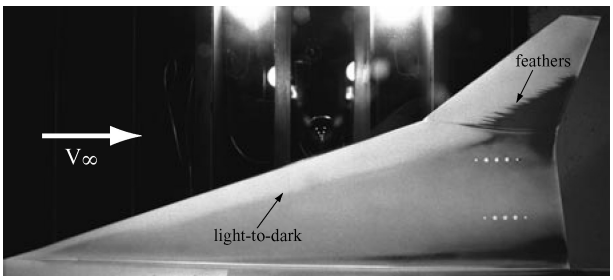

Fig. 7 Free transition sublimation image, upper surface.

inboard portion of the wing, for disk heights of 0.010 in. (0.254 mm) and greater, turbulent wedges are visible downstream of the disks (Fig. 4). For the smaller disk heights, wedges were sometimes visible, especially behind the isolated disks. The transition line was placed at the beginning of the wedges whenever they were visible. 2) Over both surfaces of the inboard region for free transition and on the inboard, upper surface for the smaller disk heights, turbulent wedges were not consistently visible. In these areas, transition was located where the color of the sublimation material changed from light gray, indicating laminar flow, to dark gray (where the fluorene has nearly disappeared) representing turbulent flow; see Fig. 7. 3) In the outboard region for free transition, a feathery pattern emerges in the sublimation material on both surfaces (Fig. 7). This pattern is characteristic of crossflow vortices.[18] In this case, the transition line was located by averaging through the "feathers." The sublimation images for the two smallest disk heights obtained during the second test, 0.002 and 0.004 in. (0.0508 and 0.1016 mm), raised additional issues to be discussed later.

On the upper surface, the movement of the transition front with increasing disk height is clearly different in the inboard and outboard regions; see Fig. 8a. Transition is delayed for all disk heights over most of the inboard region. Near the wing–body junction ($y = 1.5$ in. or 3.81 cm), transition occurs close to the leading edge for all trip configurations, including the no-trip case, perhaps due to contamination of the wing attachment line by the turbulent boundary layer on the fuselage. Outboard, transition moves abruptly forward from its natural location for even the smallest disk height, 0.006 in. (0.152 mm) and becomes prompt for trip heights of 0.010 in. (0.254 mm) and greater. The entire lower surface behaves similarly to the upper, outboard wing panel in that nearly prompt transition occurs for all disk heights; see Fig. 8b.

Reanalysis

The reanalysis of trip drag began with a quantitative evaluation of the laminar run correction for each trip height tested. The wind-tunnel data were "corrected" to match a standard condition corresponding to fully turbulent flow, i.e., transition located at the leading edge. Two skin-friction drag estimates are required, for a turbulent boundary layer and for a mixed laminar–turbulent layer with transition at the measured location. The difference between these two quantities is the correction to be added to the measured drag for each trip height.

To evaluate the correction, the boundary layer is assumed to develop under freestream conditions on an adiabatic flat plate with zero pressure gradient. Turbulent skin friction was computed using the van Driest flat-plate formula for total drag.[19,20] Skin-friction drag for the mixed laminar–turbulent case is based on a standard iterative procedure that matches laminar and turbulent momentum thickness at the transition location. The laminar layer's skin-friction coefficient is from the Blasius solution, using Eckert's reference temperature to account for compressibility.[21] Momentum thickness is related to the average skin-friction coefficient by the momentum-integral equation for a two-dimensional, zero-pressure-gradient boundary layer. The skin friction for the mixed case is actually that for a turbulent boundary layer, starting from a "virtual" origin, whose momentum thickness matches the laminar layer's at the transition location. Each surface of the wing is divided into 10 or more rectangles for computational purposes. Previous comparisons of skin-friction drag estimates on several HSCT wings at the supersonic cruise condition showed that flat-plate approximations were within 10% of Navier–Stokes computations. Based on these analyses, using the zero-pressure-gradient, flat-plate estimates as a correction methodology was considered to be sufficient.

A portion of the laminar run correction uncertainty, resulting from the way that the transition front is mapped out, can be estimated. Several of the runs were reanalyzed using different, plausible criteria for selecting transition location. In addition, some trip heights were repeated in the second test entry. On the basis of these repeated measurements, we feel that an uncertainty estimate of ± 0.2 drag counts (at a subjective 95%-confidence level) is reasonable. This includes both a possible bias error, arising from the use of the earliest identifiable wedge location, and a mix of bias and precision errors from the choice of images within a run series. Finally, the compressible, turbulent skin-friction formula on which the turbulent and mixed laminar–turbulent calculations are based is probably not accurate to better than 5–10%, even for a true flat-plate boundary layer. This suggests a possible bias error in the laminar run corrections on the order of a few tenths of a count.

The strongly scrubbed appearance of the sublimation material immediately downstream of the disks raises the question of whether there might be a systematic effect (bias) caused by altered skin friction in the wake. Drake[15] shows that there is indeed an effect: the C_f values in the near wake vary from laminar to roughly twice turbulent levels. The skin friction in the wake eventually becomes indistinguishable from a turbulent boundary layer downstream of a two-dimensional trip. For this study, the wake was assumed to be either laminar or turbulent; a more sophisticated treatment awaits further data on the skin-friction distribution downstream of an array of disk trips.

Skin-friction drag estimates are given in Table 1 for the free transition and $k = 0.012$ in. (0.305 mm) nominal trip height cases. The correction for laminar run is not an insignificant portion of the drag

Table 1 Skin-friction drag estimates and laminar run correction

	C_D		
k, in./mm	Turbulent	Mixed	Laminar run correction
0.0	0.003617	0.003041	0.000576
0.0122/0.310	0.003586	0.003414	0.000172

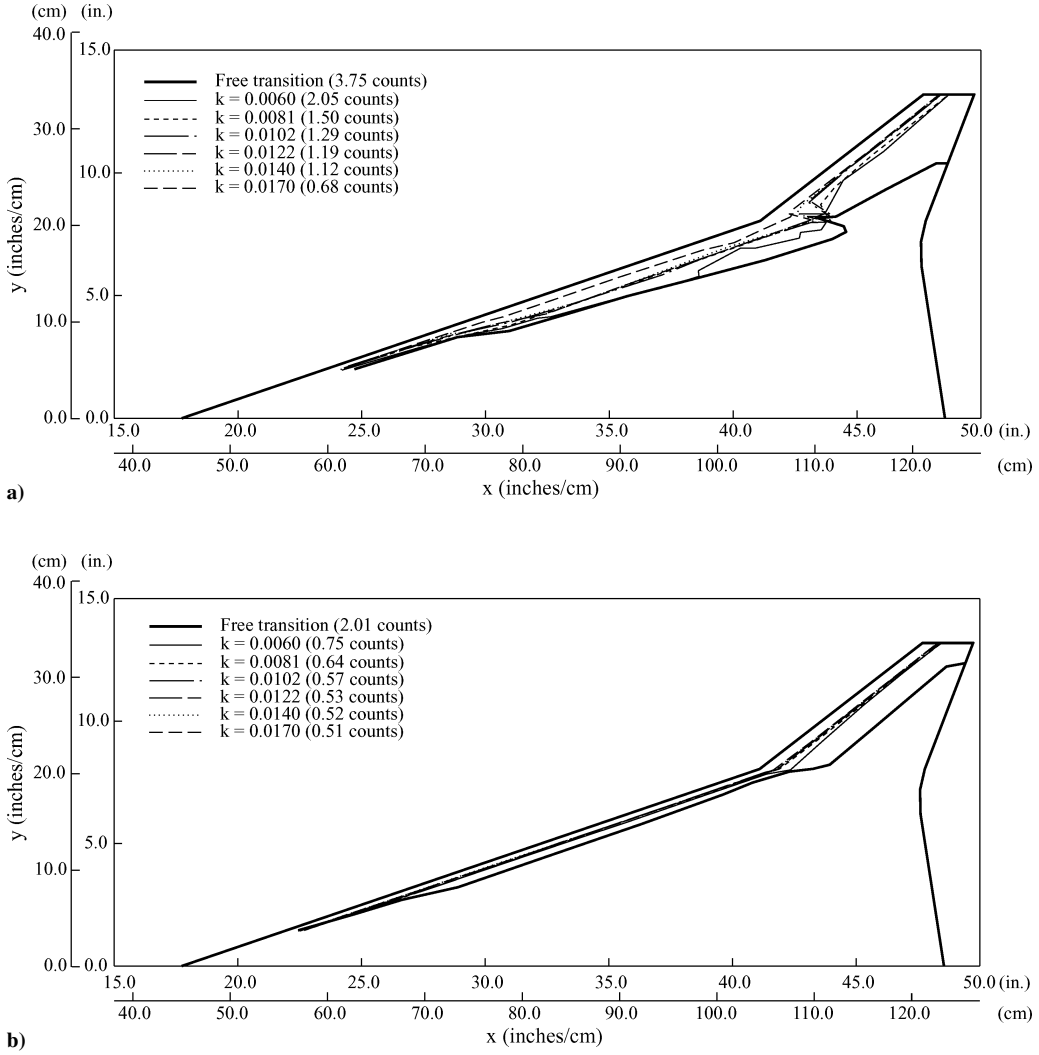

Fig. 8 Summary of measured transition locations (and laminar run corrections): a) upper and b) lower surface.

due to friction. The minimum laminar run correction corresponding to laminar flow from the leading edge to the disk location is 0.89 counts. That the two fully turbulent values do not quite agree is an artifact of the measuring process; the inboard boundary of the corrected region in the flow visualization images was not perfectly consistent. The laminar run corrections are not affected because the turbulent and mixed results for each case are based on exactly the same portion of the wing.

With laminar run corrections applied, the data can now be reanalyzed for trip drag. Both the uncorrected and corrected values are plotted as a function of disk height in Fig. 9. Note that the data have been interpolated at a consistent angle of attack of 3.5 deg to match the conditions of the flow visualization. For the corrected data, the measurement uncertainty of the laminar run correction has been added to the precision error in the root-sum-squares sense. The corrected drag curve is similar to that obtained by Vaucheret.[8] The first three data points have almost the same value of drag; we tentatively identify this region as a drag plateau; the average C_D of the three points is 0.011774. For k larger than 0.008 in. (0.203 mm), on the order of the boundary-layer thickness or greater, a linear least-squares curve with a slope equal to 0.0453/in. (0.00178/mm) appears to represent the data well, as would be expected, per Braslow et al.,[7] for cylindrical trip elements. Following Vaucheret's analysis, there is no trip drag for disk heights within the plateau region. Beyond the plateau, the trip drag is the difference between the linear fit and the

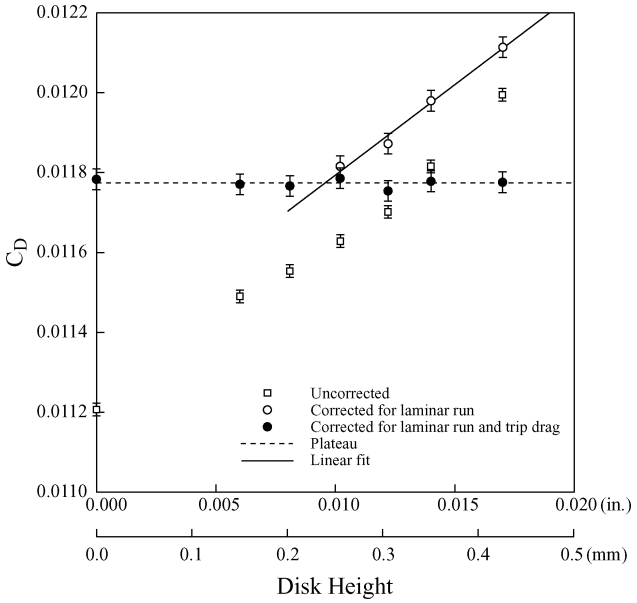

Fig. 9 Corrected and uncorrected cruise drag as a function of disk height (first wind-tunnel test).

Table 2 Measured and corrected values of cruise drag

k, in./mm	C_D (wind tunnel)	Laminar run	Trip drag	C_D (corrected)
0.0	0.011207	0.000576	0.0	0.011783
0.0122/0.310	0.011702	0.000172	−0.000120	0.011754

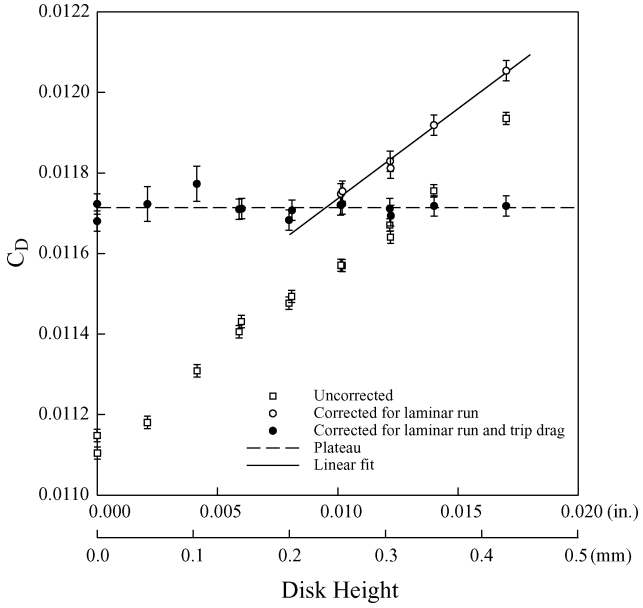

Fig. 10 Corrected and uncorrected cruise drag as a function of disk height (merged data from both wind-tunnel tests, offset to match plateaus).

plateau value. For each disk height, the trip drag is subtracted from the drag corrected for laminar run to obtain the final, corrected drag of the wing/body configuration at the cruise condition.

Measured and fully corrected cruise drag values for two cases are given in Table 2 along with their laminar run and trip drag corrections. For $k = 0.0122$ in. (0.305 mm), a typical value, the laminar run and trip drag corrections are of similar magnitude but opposite sign. Thus, although neither correction is negligible, in this case the two roughly cancel. The final, corrected values are within 0.2 counts of the plateau level. Two significant differences exist between the present results and those of Vaucheret.[8] In Vaucheret's experiment, 1) prompt transition was observed for sufficiently large trips, and 2) the trips began to create additional drag only after they were large enough to induce prompt transition. In the present case, transition is never prompt on the inboard, upper wing surface where the pressure gradient is highly favorable. A laminar run correction is thus required for all disk heights, and there is no neat division between the "laminar run correction required" and "trip drag" regimes.

Second Test Entry

The second wind-tunnel test provided an opportunity to extend the database to smaller trip heights and to verify the trends observed in the first test. In particular, it was hoped that the addition of the smaller disk heights would confirm the presence of a drag plateau between $k = 0$ and 0.008 in. (0.203 mm). The results from the two tests exhibit consistent trends but are offset from each other by an amount several times larger than the uncertainty represented by the error bars. We attribute this offset to the use of different force balances. The absolute accuracy (bias uncertainty limit) of the Langley UT65 balances is about ±0.75 counts (95% confidence); this is large enough to account for the discrepancy. The approach taken was to fit the two data sets separately and then combine them; see Fig. 10.

For trip heights through $k = 0.008$ in. (0.203 mm), the corrected data from the second test exhibit more scatter than from the first test but are still consistent with a drag plateau. The "new" points at $k = 0.002$ and 0.004 in. (0.0508 and 0.102 mm) are plotted with more generous error bars to reflect difficulty of the interpretation of the flow visualization images (discussed later). There was also some additional experimental uncertainty during the testing of the smaller disks heights caused by instability in the cavity pressure measurements that are used to correct the model base pressure. The five corrected data points from $k = 0.0$ to 0.008 in. (0.203 mm) were averaged to arrive at a plateau level for the second test, which was 1.20 counts lower than the previous level. The data sets were merged by offsetting each by half the difference between the two plateau levels; the merged drag plateau level is 0.011714. The data from both tests beyond the plateau are well represented by a single straight line with slope 0.0447/in. (0.00176/mm), similar to the result from the first test. The new trip drag correction for $k = 0.0122$ in. (0.310 mm) is −1.21 counts, vs −1.20 counts in Table 2. Thus, whereas the second entry provides only modest support for the hypothetical drag plateau, the impact of including these results on the estimated trip drag is negligible when the plateau model is used to analyze the combined results of the two tests.

The larger estimated errors associated with the two smallest disk heights are primarily a result of the uncertainties involved in locating transition on the upper surface. There are two issues, one related to the development of the sublimation patterns over time and the other having to do with the interpretation of the patterns. In our procedure, the transition location for each trip height is determined by studying a series of selected images taken a few minutes apart. Heretofore, the transition location has been stable for a period of time before appearing to move forward as the sublimation material finally erodes. However, the transition locations for the two smallest disk heights seem to shift forward continuously, making it difficult to identify the transition location with confidence.

Interpretation of the sublimation images presents a puzzle for the smallest disk height, $k = 0.002$ in. (0.0508 mm). The flow in the region just outboard of the break exhibits a pattern different from what was seen in either the free transition images or those of larger disk heights. Neither the feathery pattern nor wedges are seen behind the disks. The new pattern consists of two distinct lines of sublimation material extending well downstream behind each disk (Fig. 11). The ends of the lines are downstream of what appears to be the natural transition location adjacent to the isolated disk. Some flow mechanism present only for the smaller disks preserves the streaks even as the background fades. The sublimation material sprayed over the disks may also be altering the flow. The chemical coating fills in the area around the base of the disks and rounds out the disk/wing junction. In the future, it may be better to leave the leading edge and the disks themselves free of sublimation material. The transition location was chosen to be near the ends of the sublimation lines because they are consistent with the overall light-to-dark-gray pattern evident in the early images and because they are relatively stable (more so than the light-to-dark-gray pattern between the disks). The data plotted in Fig. 10 are based on average laminar run corrections representing a range of possible transition locations. The error bars reflect a doubling (to ±0.4 counts) of the uncertainty attributed to the laminar run correction. This is based on our experience in using different images in the series to estimate transition location.

The lower surface did not present any new interpretative challenges. The transition indicators described earlier were used for the new, smaller disks. It remains unclear why the anomalous behavior

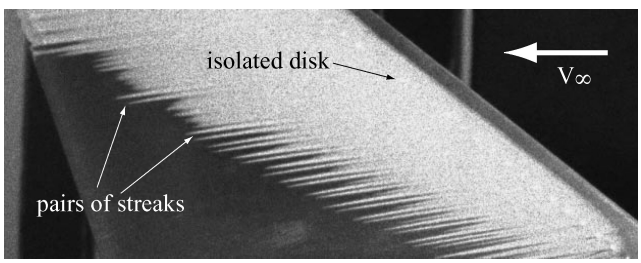

Fig. 11 Sublimation image showing distinct pairs of lines on the outboard, upper surface, $k = 0.002$ in. (0.0508 mm).

on the outboard, upper surface does not match that on the lower surface, where the pressure distribution is similar.

Discussion

Applicability of Braslow et al.'s Criteria

The transition behavior on the inboard, upper surface is distinct from both the outboard panel and the inboard, lower surface. Braslow et al.'s[7] criteria for trip sizing and location, $Re_k = 600$ for $Re_x = 2 \times 10^5$ at Mach = 2.4, appear to have been successful in effecting nearly prompt transition on the outboard wing (for immediate transition, Re_k values of 2×10^3 to 3×10^3 were required). The criteria fail, however, on the inboard, upper surface; prompt transition was not obtained even for Re_k values as large as 5×10^3. This may be due to the pressure distribution, which differs from the rest of the wing. Laminar surface pressures computed by NASA's upwind parabolized Navier–Stokes (UPS) code, which solves the parabolized Navier–Stokes equations,[22] are shown in Fig. 12 at two span stations, inboard and outboard of the planform break. The trip disk and natural transition locations are indicated. The associated boundary-layer plots showing velocity distribution and Re_k at the streamwise point in the flow corresponding to the trip location are presented in Fig. 13. For the laminar calculations, the boundary layers are resolved by approximately 20 grid points normal to the surface at the trip disk location. Compressible flat-plate results (also from the UPS code) are included for comparison. (Boundary-layer quantities based on the Blasius solution are shown to emphasize the importance of compressibility in assessing the trip height criteria: use of the incompressible properties would result in undersizing the trip by a factor of two for $Re_k = 600$.)

A striking difference between the two regions of the wing is that the pressure gradient is highly favorable around the blunt, inboard leading edge followed by a region of nearly constant pressure, whereas outboard the pressure gradient is continuously favorable. In addition, for a given physical trip height, Re_k is smaller for the inboard, upper surface than for the outboard wing. Both factors suggest that the upper, inboard surface will be more difficult to trip. Braslow et al.'s[7] criteria may have been more successful outboard because their work was based on a flat-plate boundary layer. Here, the outboard wing boundary layer resembles that of a flat plate (Fig. 13), but on the inboard, upper surface, the boundary-layer thickness is greater and the values of Re_k are less than those of the flat-plate solution. Because of these differences, the apparent breakdown of Braslow et al.'s correlation in the inboard region is not surprising.

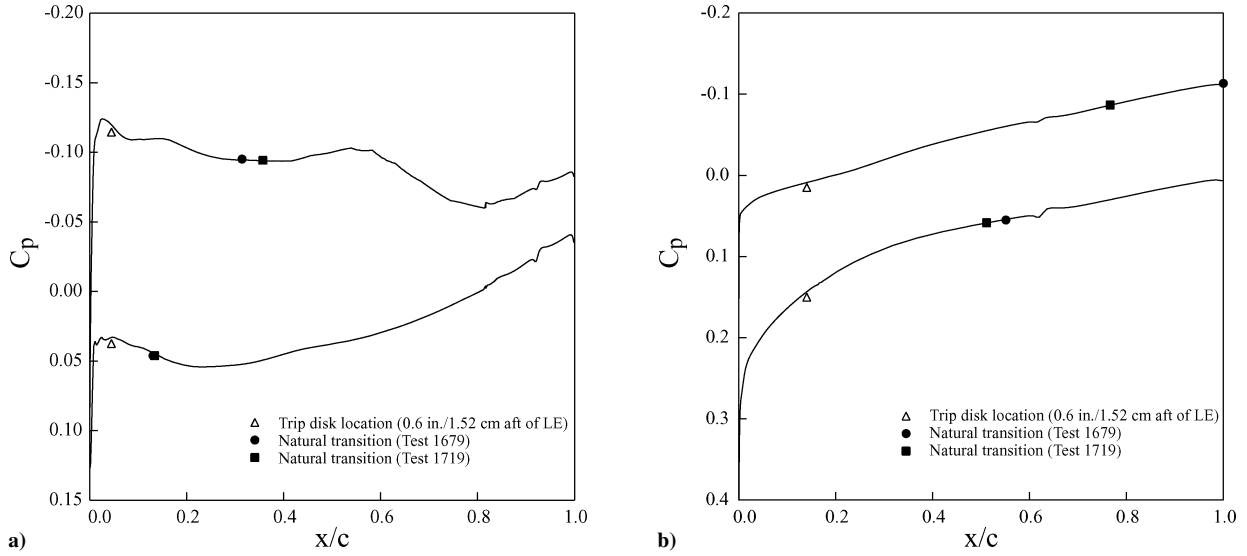

Fig. 12 Surface pressure coefficient computed by UPS: a) inboard station ($2y/b = 0.43$) and b) outboard station ($2y/b = 0.81$).

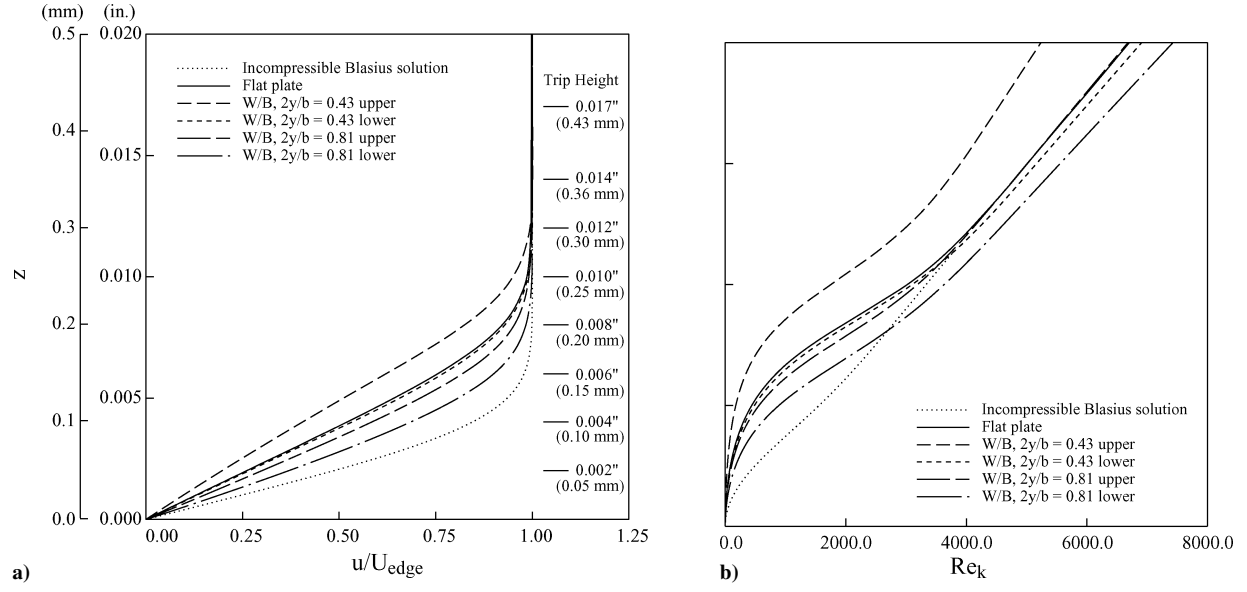

Fig. 13 Computed (UPS) boundary-layer properties at trip location, $x = 0.6$ in. (1.52 cm): a) normalized velocity distributions and b) Reynolds number based on height above surface.

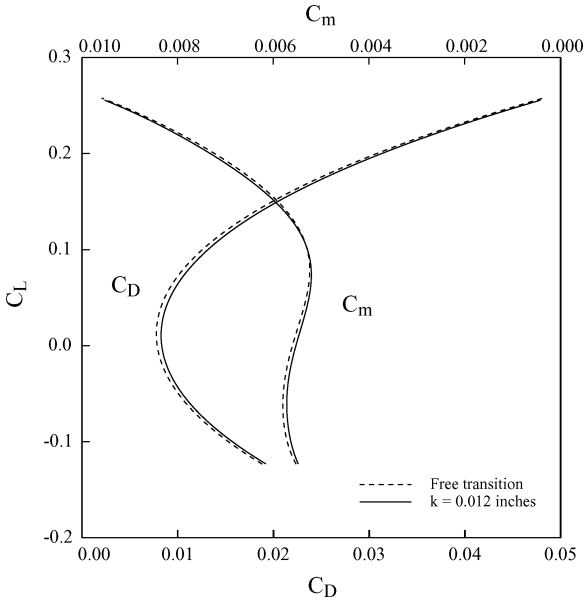

Fig. 14 Drag polar and pitching moment curves represented by seventh-order polynomial fits to the free transition and $k = 0.012$ in. (0.305 mm) data.

Prompt transition is obtained on the inboard, lower surface for disk heights on the order of the boundary-layer thickness. Although there is a similarly favorable pressure gradient, the flow does not accelerate around the blunt leading edge as much on the lower surface as it does on the upper (Fig. 12a). In addition, the computed boundary-layer properties on the lower surface resemble those of the flat plate (Fig. 13). Last, the natural transition location on the lower surface is closer to the leading edge than on the upper surface. All of these factors seem to facilitate prompt transition to turbulent flow using trip disks.

Is It Necessary to Trip the Flow?

The evidence for a drag plateau in the corrected data is consistent with Vaucheret's[8] observations at similar Mach and Reynolds numbers. These trends suggest that it may not be necessary to trip the flow at all, at least for conditions similar to the present work. Vaucheret's results suggest this possibility, but he did not pursue this alternative. Some further analysis is necessary before concluding that tripping the boundary layer is superfluous.

The shapes of the drag polars for the model with and without trips applied are smooth and nearly parallel, separated by about five drag counts (Fig. 14). No irregularities are evident that would suggest any erratic behavior of the transition location or flow separation for the free transition case. With the proper laminar run and trip drag corrections, both polars give the same fully corrected drag, at least around the cruise point. (Additional work will be required to determine how many points of the polar must be examined for laminar flow correction, which will in general vary with angle of attack.) Pitching moment, also shown in Fig. 14, is a second aerodynamic characteristic that could be affected by the extent of laminar flow or the presence of separation. The slight discrepancy between the curve fits to the data is less than the scatter obtained between repeat runs. Thus, with suitable corrections for laminar run, both the drag and pitching moment data confirm that the free transition data are valid for this configuration.

Conclusions

Two wind-tunnel tests were conducted to measure the cruise performance of a supersonic transport. Different parts of the wing, characterized by leading-edge radius, sweep angle, pressure distribution, and perhaps other factors, exhibit distinct transition behavior. It is imperative to determine the location of transition for each trip configuration using flow visualization, or perhaps some other method. Neither Braslow et al.'s criteria for required trip height nor inspection of the drag polar suffices to ensure that prompt transition has been obtained. Prompt transition was obtained on both surfaces of the outboard wing and on the lower, inboard surface for Re_k values on the order of 2×10^3 to 3×10^3, but transition was always delayed on the inboard, upper surface regardless of Re_k. A correction for the effect of laminar run must be added to the drag for the different trip heights, to put all of the data points on a common footing with regard to skin friction, before any further analysis can be performed.

It was discovered that the interpretation of sublimation images can be misleading. The strongly scrubbed regions just behind the trips for all but the smallest disk heights are easily mistaken for prompt transition. This can be avoided by obtaining a series of images (until the sublimation material has nearly disappeared) and by leaving a few disks isolated so that the development of a transition wedge in their wakes is discernible.

The results of the present work are consistent with those of Vaucheret and others who found evidence that a drag plateau exists at supersonic speeds. Once the effect of laminar run is accounted for, small trip disks add no drag. Above this plateau region, trip drag varies linearly with disk height. The various schemes for deducing trip drag by fitting the large-trip data and extrapolating to zero height will produce erroneous results because they ignore the plateau.

For some wind-tunnel model configurations and testing conditions, it may not be necessary to trip the flow at all. Flow visualization, possibly at several angles of attack, would still be required to measure transition location to account for the effects of laminar run.

Acknowledgments

The authors acknowledge with gratitude the contributions of Gelsomina Cappuccio (NASA Ames Research Center), Kevin Mejia (Boeing Commercial Airplanes), and Jerry Allen (NASA Langley Research Center), who assisted with the wind-tunnel tests, and Scott Lawrence (NASA Ames Research Center), who provided the UPS computations. We benefited from helpful discussions with Paul Vijgen and Robert Patton of Boeing Commercial Airplanes and Russ Westphal and Aaron Drake of Washington State University.

References

[1]Whitehead, A. H., Jr., "Status of NASA High-Speed Research Program," *Fluid Dynamics Research on Supersonic Aircraft*, NATO Research and Technology Organization Educational Notes 4, May 1998, pp. 10-1–10-20.

[2]Jackson, C. M., Jr., Corlett, W. A., and Monta, W. J., "Description and Calibration of the Langley Unitary Plan Wind Tunnel," NASA TP 1905, Nov. 1981.

[3]Foster, C. B., "Method of Applying Turbulators to Wind Tunnel Models," U.S. Patent No. 4,537,647, Aug. 1985.

[4]Russo, G. P., "Techniques for Boundary Layer Tripping and Control," *Boundary Layer Simulation and Control in Wind Tunnels*, AGARD Advisory Rept. 224, April 1988, pp. 80–90.

[5]Loftin, L. K., Jr., "Effects of Specific Types of Surface Roughness on Boundary-Layer Transition," NACA Wartime Rept. L-48. (Originally published as NACA ACR L5J29a, Feb. 1946.)

[6]Abbott, I. H., and von Doenhoff, A. E., "Effect of Surface Irregularities on Drag Characteristics," *Theory of Wing Sections*, Dover, New York, 1959, pp. 157–187.

[7]Braslow, A. L., Hicks, R. M., and Harris, R. V., Jr., "Use of Grit-Type Boundary-Layer-Transition Trips on Wind-Tunnel Models," NASA TN D-3579, Sept. 1966.

[8]Vaucheret, X., "Artificial Initiation of the Supersonic Transition," NASA TT F-11,558, Feb. 1968. (Originally published as "Declenchement Artificiel de la Transition en Supersonique," *La Recherche Aerospatiale*, No. 120, Sept.–Oct. 1967, pp. 25–32.

[9]Fallis, W. B., "On Distributed Roughness as a Means of Fixing Transition at High Supersonic Speeds," *Journal of the Aeronautical Sciences*, Vol. 22, No. 5, 1955, p. 339.

[10]Daugherty, J. C., "Wind-Tunnel/Flight Correlation Study of Aerodynamic Characteristics of a Large Flexible Supersonic Cruise Airplane (XB-70-1): I—Wind Tunnel Tests of a 0.03-Scale Model at Mach Numbers from 0.6 to 2.53," NASA TP 1514, Nov. 1979.

[11]Coleman, H. W., and Steele, W. G., Jr., "Confidence Intervals in Sample Populations," *Experimentation and Uncertainty Analysis for Engineers*, 1st ed., Wiley, New York, 1989, pp. 27–30.

[12]Main-Smith, J. D., "Chemical Solids as Diffusible Coating Films for Visual Indications of Boundary-Layer Transition in Air and Water," Aeronautical Research Council, Repts. and Memoranda No. 2755, London, Feb. 1950.
[13]Owen, P. R., and Ormerod, A. O., "Evaporation from the Surface of a Body in an Airstream (with Particular Reference to the Chemical Method of Indicating Boundary-Layer Transition), Aeronautical Research Council, Repts. and Memoranda No. 2875, London, Jan. 1954.
[14]Kennelly, R. A., Jr., and Goodsell, A. M., "Skin Friction and Transition Location Measurements on Supersonic Transport Models," *Proceedings of the 9th International Symposium on Flow Visualization*, edited and published by G. M. Carlomagno and I. Grant, Edinburgh, 2000, pp. 160-1–160-18.
[15]Drake, A., "Effects of Cylindrical Surface Protrusions on Boundary Layer Transition," Ph.D. Dissertation, School of Mechanical and Materials Engineering, Washington State Univ., Pullman, WA, May 1998.
[16]Gregory, N., and Walker, W. S., "Part I: The Effect of Transition of Isolated Surface Excrescences in the Boundary Layer," Aeronautical Research Council, Repts. and Memoranda No. 2779, London, Oct. 1951.
[17]van Driest, E. R., and McCauley, W. D., "The Effect of Controlled Three-Dimensional Roughness on Boundary-Layer Transition at Supersonic Speeds," *Journal of the Aerospace Sciences*, Vol. 27, No. 4, 1960, pp. 261–271.
[18]Obara, C. J., "Sublimating Chemical Technique for Boundary-Layer Flow Visualization in Flight Testing," *Journal of Aircraft*, Vol. 25, No. 6, 1988, pp. 493–498.
[19]van Driest, E. R., "Turbulent Boundary Layer in Compressible Fluids," *Journal of the Aeronautical Sciences*, Vol. 18, No. 3, 1951, pp. 145–160.
[20]van Driest, E. R., "The Problem of Aerodynamic Heating," *Aeronautical Engineering Review*, Vol. 15, Oct. 1956, pp. 26–41.
[21]Eckert, E. R. G., "Engineering Relations for Friction and Heat Transfer to Surfaces in High Velocity Flows," *Journal of the Aeronautical Sciences*, Vol. 22, No. 8, 1955, pp. 585–587.
[22]Lawrence, S. L., Tannehill, J. C., and Chaussee, D. S., "Development of a Three-Dimensional Upwind Parabolized Navier–Stokes Code," *AIAA Journal*, Vol. 28, No. 6, 1990, pp. 971, 972.

J. Hermanson
Associate Editor